Dual-beam polarimeter for measuring birefringent waveplates

Edward A. West, Jason Porter and Matthew Lewis[a]

NSSTC/NASA/MSFC
SD50
Huntsville, Alabama
35805
E-mail: edward.west@msfc.nasa.gov

Abstract

1. Introduction

Waveplates are required to measure the complete Stokes vector (I, Q, U, and V where I is intensity, +Q is linear polarization at 0°, +U is linear polarization at 45° and +V is right circular polarization) but limit the accuracy of the polarization measurements if the systematic errors are not known and minimized. While electro-optic modulators, such as KD^*Ps (potassium di-dueterium phosphate) and LCDs (liquid crystal devices), are used as variable waveplates and can reduce intensity crosstalk when the polarization source is not stable, their electrodes and crystal properties can degrade with time, making them poor candidates for instruments requiring long-term stability. Crystalline waveplates, such as quartz and magnesium fluoride (MgF_2), are stable but can introduce systematic errors.

This paper describes two dual-beam polarimeters that have been developed to measure the retardance of waveplates in both the UV and visible wavelength regions. Section 2 will describe the two polarimeters , Section 3 will develop the observing program and calibration procedures required to make retardation measurements and Section 4 will describe the waveplate errors that affect the retardation measurements and how those errors must be minimized.

2. Instrumentation to measure retardance

A dual-beam polarimeter is simply an analyzer that separates the incident light into two polarization paths. While dielectric polarizing beamsplitters could be used, they have a narrow wavelength band and poor polarization resolution when compared to birefringent crystals. In order to develop "broad-band" measurements, a beam-splitting Glan-Thompson analyzer is used in the visible light measurements while a MgF_2 double Wollaston analyzer is used in the UV measurements. While both analyzers use birefringent properties to separate the two polarization paths, the Glan-Thompson uses the cut angle of the calcite crystal to reflect the ordinary ray while the double Wollaston uses the difference in the refractive indices of the MgF_2 crystal to separate the ordinary and extra-ordinary rays. The Glan-Thompson approach is much better for imaging applications and can cover a wavelength range from 400-2000nm[2]. Using MgF_2, the double Wollaston analyzer can be used in our vacuum UV measurements with a wavelength range from 140-360nm[3].

---

[a] Currently at: ????

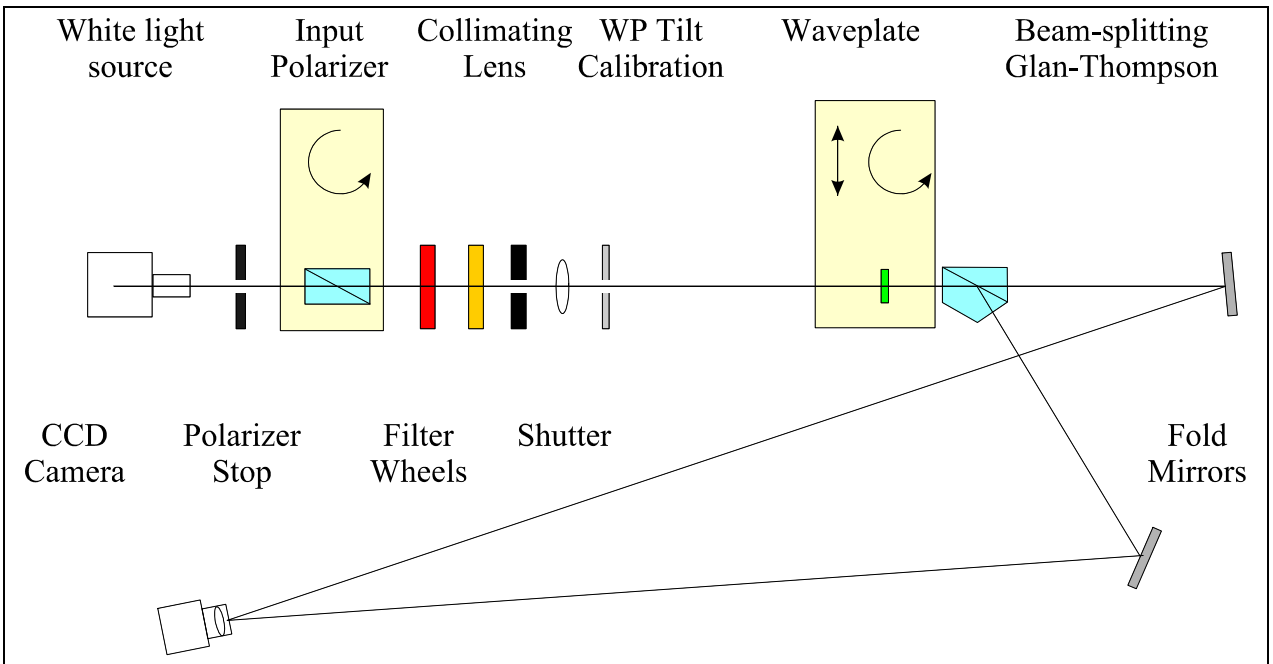

Figure 1. Optical schematic of the GT/visible light test

While dual-beam polarimeters have the advantage of measuring both the polarization and intensity in a single measurement, it has additional calibration requirements to eliminate any gain differences in the two optical paths. This will be described in Section 3. The dual-beam approach can (1) make the same measurements as a single beam polarimeter but with two channels, see Section 3 and (2) eliminate intensity crosstalk when the source is changing rapidly. Although measurements using a Soleil-Babinet will be used in the discussion of the retardation measurements (Section 4 and 5), this technique has been described elsewhere[1] and will not be discussed here. This measurement technique is similar to the single channel measurements but uses a variable waveplate (Soleil-Babinet compensator) to determine the retardance of the unknown waveplate. The main difference in the single channel measurements and the Soleil-Babinet measurements is the light source: a quartz tungsten lamp with an intensity monitor for the single channel measurements and a HeNe laser for the Soleil-Babinet compensator measurements. Most of the calibration issues are the same for the two techniques and will discussed in Section 3.

2.1 Visible light, Glan-Thompson polarimeter

Many of the reasons for developing the Glan-Thompson polarimeter were based the experience gained in an earlier development program to measure the waveplates for the MSFC Experimental Vector Magnetograph[1]. In that program, a multi-line HeNe laser, a Soleil-Babinet compensator and a PM tube were used to measure the retardance of zero-order quartz and achromatic quartz/MgF_2 waveplates. Although the program was able to achieve the desired resolution and model the waveplate errors, the data acquisition was very labor intensive. This was due to the mechanical tuning of the Babinet compensator and laser, and the instability of the HeNe laser which required a large number of measurements to reduce the intensity crosstalk. While the HeNe laser provided an absolute wavelength calibration (HeNe lines of 5435, 5941,

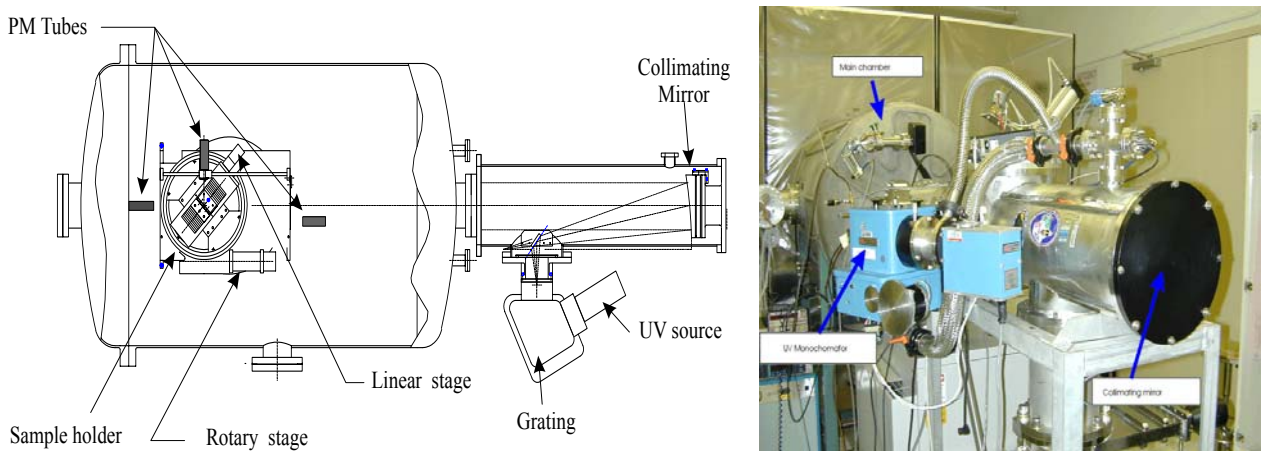

FIGURE 2. NSSTC VUV TEST CHAMBER

6040, 6119 and 6328 Å), these measurements had to be extended to one of the primary wavelengths, 5250Å.

The Glan-Thompson dual-beam polarimeter was developed to automate the data acquisition, eliminate intensity crosstalk and extend the wavelength range. Based on the waveplate errors that were identified in the previous program, the data system was developed to measure not only the normal incident retardation but to look at field of view and optic axis tilt errors. These will be discussed in Section 4.

Figure 1 shows the optical schematic of the beam-splitting Glan-Thompson dual-beam polarimeter. The light source is an Oriel quartz tungsten halogen lamp with a radiometric power supply. This lamp provides a uniform irradiance over a large spectral range (3000-25000Å). In addition a light intensity controller is used to reduce short term variations in the irradiance output to minimize the intensity crosstalk in the single beam retardation measurements (Section 3.1). Two computer controlled filter wheels insert narrowband filters that cover the visible spectrum. The first set of narrowband filters are the HeNe filters that were used in the Soleil-Babinet compensator measurements while the second filter wheel extended the wavelength range from 4800 to 7250Å. Although the lamp housing has a lens to collimate the source, a stop and additional lens is required to reduce the beam expansion from the extended source. A calibration stop is placed ~700mm from the waveplate and is used to observe and control the tilt of the waveplate. The waveplate is mounted to a linear stage which will remove it for calibration measurements and a rotary stage to make measurements as a function of the "fast axis" position[†]. Fold mirrors then redirect the two polarization paths from the Glan Thompson analyzer onto a single CCD camera.

For the Glan-Thompson polarizers, the cut angle of the calcite is such that the ordinary ray is totally reflected at the interface while the extra-ordinary ray is transmitted undeviated through the polarizer. The input polarizer is a standard Glan-Thompson where the ordinary ray

[†] MgF_2 is a positive uniaxial crystal making the extra-ordinary index larger than the ordinary. Therefore the extra-ordinary crystal direction, which is the optic axis direction (not to be confused with the optical axis), would be considered the slow axis; ordinary the fast axis. For low-order retarders, with a fast and slow axis for each crystal, the waveplate fast axis can be confusing but is simply used to designate the "apparent" orientation of the optic axis of the waveplate.

is absorbed while the analyzer is a beam-splitting Glan-Thompson. These polarizers can achieve extinction ratios greater than 10^{-5}. The input Glan-Thompson is mounted to a rotary stage so that both polarization beams from the beam-splitting analyzer can be used in the single-beam polarimeter measurements (Section 3.1).

2.2 Ultraviolet double Wollaston polarimeter

In order to extent our retardance measurements into the vacuum UV, a second dual beam polarimeter was developed. Figure 2 shows the test chamber where these UV measurements are made. This vacuum UV spectrophotometric test facility was been developed at the NSSTC/MSFC for measuring the optical properties (transmittance, reflectance and polarization) of test samples in the wavelength range from 1150 Å through the visible. This facility was used to test the Ultraviolet Imager for the International Solar Terrestrial Physics Mission and for the Wide Imaging Camera for the IMAGE Mission. For VUV optics, contamination is a serious concern. In order to minimize exposure of test optics to contamination, the spectrophotometric system is contained in a stainless steel vacuum chamber maintained in a class 10K clean area. A cryogenic hydrocarbon-free pumping system is used to avoid contamination. The vacuum system operates with a base pressure in the 10^{-7} torr range. For VUV measurements, a high-pressure arc discharge deuterium lamp is used as the source. Because of its continuum output in the 1150-3700Å range, this source is used to scan the transmission, reflection and polarization characteristics of the SUMI optics in the CIV and MgII wavelength bands. A 0.2m vacuum monochromator, with a concave holographic grating (1200 lines/mm) coupled to a 76.2cm focal length collimating UV enhanced mirror system, produces a 10.2cm monochromatic collimated incident beam. Two vacuum compatible linear stages and two rotational stages are used to position the detectors, optical components and test samples during the calibration and testing process.

In order to make high resolution polarization measurements over an extended UV wavelength range (1400-3600Å), a double Wollaston MgF_2 polarizer is used as the analyzer to the dual-beam polarimeter while a Rochon MgF_2 polarizer is the input polarizer. Instead of using reflection to separate the two beams as in the Glan-Thompson approach, the double Wollaston (and Rochon) approach is to use refraction of the ordinary and extra-ordinary rays to separate the two linear polarizations. Due to the absorption characteristics of MgF_2 and the length of the Rochon and double Wollaston polarizers, limit this polarimeter to ~1300Å. Although blocking filters could be used to extend the wavelength range, the upper limit (~3600Å) is set by the multiple-order contamination of the monochromator.

Figure 3 shows the test setup for the VUV polarimeter. An aperture stop limits the size of the 10 cm collimated beam to 2mm. A Rochon polarizer follows the aperture stop and is mounted to a rotary stage. After the Rochon polarizer a calibration stop is used to align the tilt and rotation axis of the waveplate that is being tested. This waveplate is also mounted to a rotary stage to position the fast axis and a linear stage is used to remove the waveplate for calibration measurements. Finally a double Wollaston polarizer is used as the dual-beam analyzer. Following the analyzer is a Hamamatsu UV camera system.

With the large changes in the birefringence of MgF_2 over this wavelength range, the angular beam separation between the ordinary and extra-ordinary rays in the double Wollaston analyzer peaks at ~6.9° near 1500Å and decreases to ~6.0° at 3000Å[3,4]. Therefore the distance and orientation of the Hamamatsu (1024x256, 24um pixels) from the analyzer is optimized to cover the 1300-3600Å wavelength range.

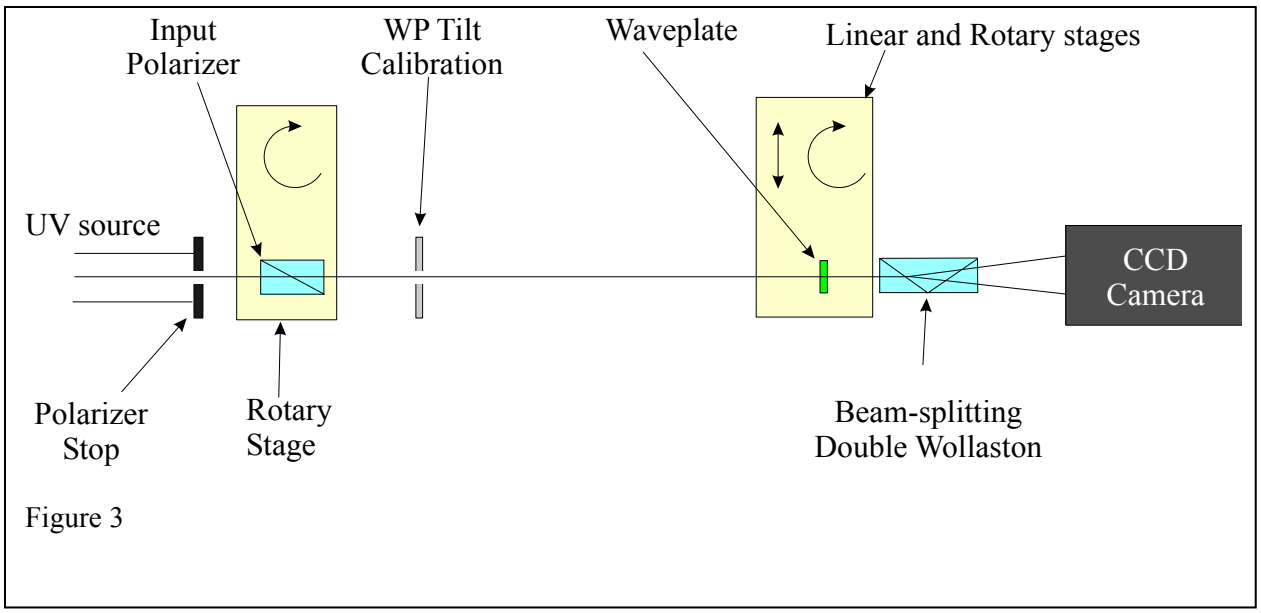

Figure 3

Although the calibration procedures for the instrumental polarization are the same for the VUV and visible light polarimeters, the instrumental polarization for the VUV system is from the grating and fold mirrors in front of the Rochon polarizer (Figure 2) while the source of instrumental polarization for the visible light polarimeter are the fold mirrors following the beam-splitting Glan-Thompson analyzer. Also the deuterium source does not have an intensity feedback system to stabilize its output which increases the intensity crosstalk in the single beam measurements.

3. Observing program

In order to discuss the errors associated with both the instrumentation, the retardation measurement and the modeling (Section 5), a waveplate that was developed for a UV magnetograph (SUMI: Solar Ultraviolet Magnetograph Investigation) will be used to demonstrate how the field-of-view, optic axis alignment, and wavelength affect the retardation mesurements. Since a discussion of the UV magnetograph can be found elsewhere, the next section will only describe the optical interface of the waveplate (angle of incidence of the chief ray and field of view defined by the marginal ray) and the retardation versus wavelength characteristics for this waveplate design.

3.1 Longitudinal waveplate design

Although SUMI has several waveplate designs that are based on different scientific observing programs, the waveplate that will be described in this paper was developed to optimize the circular polarization measurements at 1550Å (CIV 2s-2p emission lines) and 2800Å (MgII *h* and *k* emission lines). Since SUMI will be launch as part of a sounding rocket payload, the observing time is limited so that the selected waveplate must be optimized for a particular observing program. Therefore this waveplate design was developed for weak active region, longitudinal magnetic field measurements. Since the CIV emission is approximately 3 orders of magnitude lower than the MgII emission and the Zeeman effect is inversely proportional the wavelength, the design goal for this waveplate was quarterwave retardance at CIV and as close

to quarterwave at MgII as possible. Although achromatic waveplate designs are still being pursued, the number of birefringent crystals that transmit to 1500Å are limited. Therefore, using the birefringence properties of MgF_2, a single crystal design was developed for a 2^{nd} order quarterwave retardance (N*360-90=630°, N=2) at 1550Å which would produced a quarterwave retardance (~270°) at 2800Å. The extra photons at MgII will make up for any loss in the polarization efficiency of the waveplate. Total thickness of this waveplate is 2.3mm. Since this is a low-order design using a single birefringent crystal, the change in retardation with temperature can be neglected.

3.2 Retardance measurements: on-axis

This section will describe the instrumentation and observing programs that were used to measure the retardance on the SUMI longitudinal waveplate (WP7). Although the Soleil-Babinet compensator has been describe elsewhere, a small discussion of its advantages and disadvantages is included for comparison with the dual-beam polarimeter. Except for the calibration procedures, the same measurements obtain in the dual-beam measurements can be used to calculate the retardance in a single-beam mode. This section will describe the difference in the calibration procedures, develop the observing program for both the single-channel and dual channel measurements and compare the data obtain by these instruments.

3.2.1 Soleil-Babinet compensator

The Soleil-Babinet compensator has been described elsewhere[1]. Originally a PM tube was used to make the retardation measurements. PM tubes have a large dynamic range and can be used very low light levels. Since the source is a multi-line HeNe laser, a photo-diode was selected for these measurements. The primary advantage of the Soleil-Babinet compensator is the fact that it works at null points (zero light). Since all of the measurements are at the same null point, non-linear effects of the detector can be neglected. The disadvantages are: (1) the mechanical interface which makes it difficult to automate the process, (2) the variable waveplate optics are spring loaded and can bind or stick, and (3) careful tuning of the variable waveplate optics in the compensator can cause delays in the measurements and calibration runs which will allow errors to be introduced by the instability of the HeNe laser.

3.2.2 Single channel measurement

In both the single-channel and dual-channel measurements, the most important systematic error that must be minimized is the linear response of the detector with wavelength. For CCD's the most important non-linear response occurs when the pixels are near saturation. Therefore, in these measurements the CCD is operated at less than 90% of the well capacity. The gain, dark current, and integration time is programmable and a special calibration routine optimizes these settings for each of the blocking filters. At the start of each wavelength scan, a dark current (zero-illumination/shutter closed) reading is made and subtracted from each polarization measurement (Equation 1).

Calibration for the single channel measurements occur when the fast axis of the waveplate and the transmission axis of the input polarizer are aligned parallel to the transmission axes of the analyzer (ie. $\theta = 0°,180°$ for +Q channel, $\theta = 90°, 270°$ for –Q channel and, $\alpha = 0°, 90°, 180°$ and $270°$ for both channels). The retardance measurement is made when α is equal to $45°, 135°, 225°$ and $315°$. In a perfect world only one of these angles is required but, due to mechanical alignment errors of the waveplate with respect to the optical axis of the test setup and

$$da_c(\alpha,\theta) := a_c(\alpha,\theta) - dc \tag{1}$$

$$p(\alpha,\theta) := \frac{da_1(\alpha,\theta)}{da_1(\alpha-45,\theta)} \qquad \theta = 0°, 180°$$

$$pq(\alpha,\theta) := \operatorname{acos}\left[p(\alpha,\theta) - \left(1 - 2\cdot p(\alpha,\theta) + p(\alpha,\theta)^2\right)^{0.5}\right] \tag{2}$$

$$n(\alpha,\theta) := \frac{da_2(\alpha,\theta)}{da_2(\alpha-45,\theta)} \qquad \theta = 90°, 270°$$

$$nq(\alpha,\theta) := \operatorname{acos}\left[n(\alpha,\theta) - \left(1 - 2\cdot n(\alpha,\theta) + n(\alpha,\theta)^2\right)^{0.5}\right] \tag{3}$$

Figure 4. Equations for converting single-channel polarization measurements into retardance and 315°. dc = dark current, a_c = analyzer channel, da_c = analyzer signal, α = fast axis of waveplate, θ = transmission axis of input polarizer, c = 1 → *I*+*Q* or 2→ *I*-*Q*, pq is the retardance for the *I*+*Q* channel, nq is the retardance for the *I*-*Q* channel.

NOTE: $da_c(\alpha\text{-}45,\theta)$ are the single channel calibration measurements for: α-45° = 0°, 90°, 180° and 270°. Although these four measurements are the "same" and could be average, they are not in the data that is presented in this paper.

polishing errors that could introduce a tilt of the crystals optic axis, all four fast axis positions are required to evaluate the systematic errors in the retardation measurements. This will be discussed in greater detail in Section 3.3 and Section 4.

3.2.3 Dual-channel measurement

Since the single-channel and dual-channel measurements are the same, the only difference is in the calibration and conversion of those measurements into retardance. For the dual-channel measurement the calibration issues are related to the optical and electrical gain differences between the two polarization paths. Since the same CCD is used to simultaneously observe the two channels, the only difference in electrical gain is the pixel to pixel variation over the CCD detector. Therefore, the main difference is the instrumental polarization created by the fold mirrors following the Glan-Thompson analyzer in the visible-light tests. The calibration procedures to eliminate any difference in the response for the two channels is simply to remove the waveplate and average the signal as the input polarizer is rotated 45° to the beamsplitting analyzer. In order to eliminate any input polarization effects from the source, the gain calibration averages the measurements at θ = 45°, 135°, 225° and 315°. This calibration is done for each wavelength position. Figure 5 shows the equations that are used to convert the dual-channel measurements into retardance. The advantage of the dual-channel measurement is that both the calibration measurements (and retardance) are simultaneous eliminating Intensity

$$cg := \sum_{\theta} \frac{da_1(out,\theta)}{da_2(out,\theta)} \tag{4}$$

$$db(\alpha,\theta) := acos\left[\left|\frac{da_1(\alpha,\theta) - da_2(\alpha,\theta)\cdot cg}{da_1(\alpha,\theta) + da_2(\alpha,\theta)\cdot cg}\right|\right] \tag{5}$$

Figure 5. Dual-channel retardance equations. cg is the gain calibration when the waveplate is removed, θ is equal to 45°,135°,225° and 315° to average out the source and instrumental polarization effects. db the calculated retardance for each orientation of the waveplate (α = 45°, 135°, 225° and 315°) and for all orientations of the input polarizer (θ = 0°, 90°, 180°, and 270°).

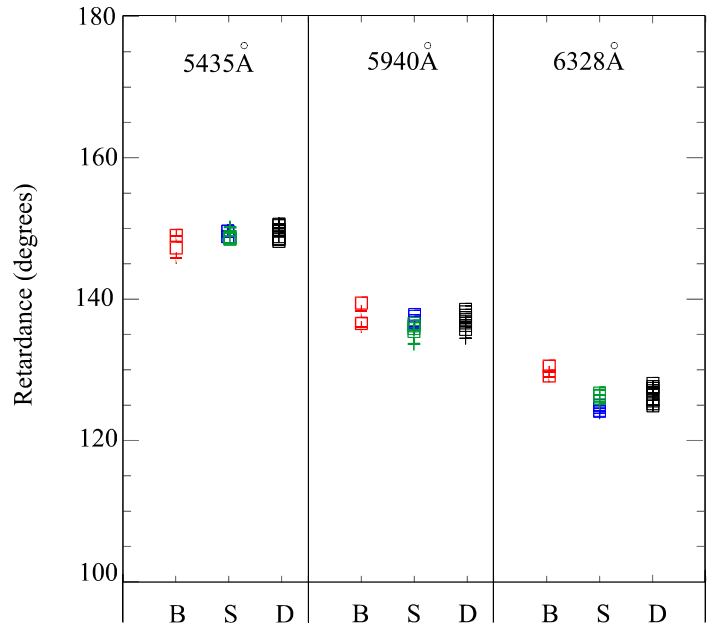

Figure 6. Comparison of retardation measurements made on the SUMI longitudinal waveplate at three wavelengths using the Soleil-Babinet compensator (B), the single channel polarimeter (S, **blue** the –Q channel, **green** the +Q channel) and the dual channel polarimeter (D) measurements. The + signs are the 45°/225° fast axis measurements, the squares are the 135°/315° measurements.

crosstalk. The single channel calibration requires two different positions of the waveplate requiring a stable source. Since the Oriel lamp has an intensity feedback, this improves the comparison between the two techniques.

3.2.4 On-axis comparison

Figure 6 compares the retardance measurements from the Babinet compensator (B), the single-channel (S) and dual-channel (D) measurements for three of the HeNe laser lines. Since two channels are measured, the +Q (pq, equation 2) and –Q (nq, equation 3) are both plotted in the single channel measurements. The single and dual channel measurements include all four orientations of the input polarizer (θ=0°, 90°, 180° and 270°) while the Soleil-Babinet measurement only uses the 90° orientation (null measurements). Figure 7 shows the same data over the wavelength covered by the narrow-band filters in the visible-light polarimeter. A straight line connects the average retardance for the single and dual-channel measurements. The most significant difference is the 6328Å measurement which shows almost a 5°difference between the single-channel and Soleil-

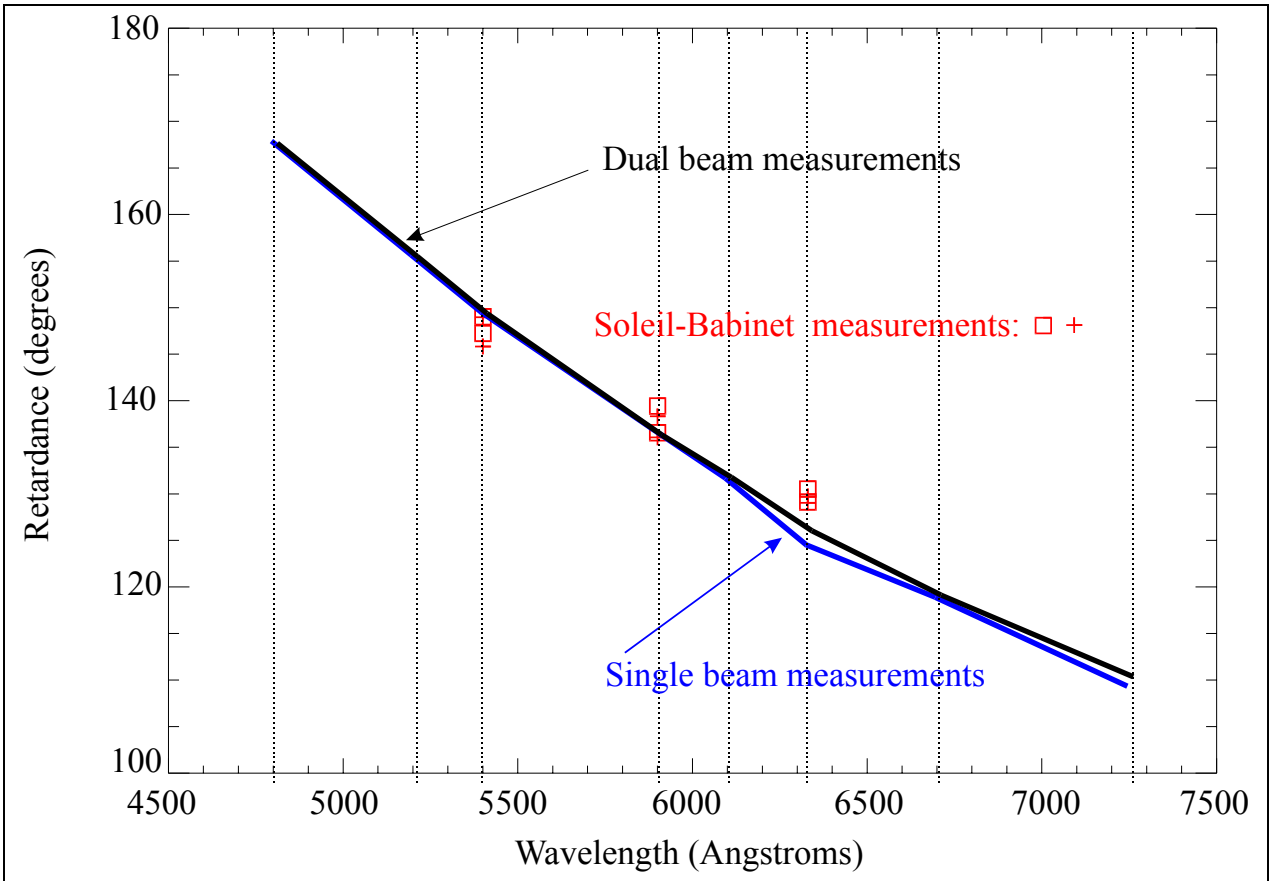

Figure 7. Retardance measurements on SUMI longitudinal waveplate WP7. The data (squares and plus signs) are the Soleil-Babinet compensator measurements(visible light/HeNe laser), the single beam curve is the average of one of the polarization channels, the dual beam curve is average of the dual beam polarization measurements. The vertical lines are the positions of the narrowband filters in the visible light measurements. Note the design goal for this waveplate was 630° retardance at 1550 Å.

Babinet compensator measurments. The next section will discuss alignment errors and their influence these retardance measurements.

3.3 Retardance measurements: 2.1° tilt

Although there appears to be a significant difference in the retardance measurements in Figure 6, some of the "noise" is optical and is related to waveplate alignment errors. This section will describe how the optic axis alignment of the MgF2 crystals and the optical alignment of the waveplate affect the retardance measurements. Based on those errors a test program has been developed to reduce the optical noise and help characterize the waveplates that are measured using the dual-channel polarimeter.

Figure 8 shows the some of the waveplate alignment positions that are possible. Ideally the optic axis (n_e) is parallel to the polished surface of the waveplate and the waveplate is mounted in the holder such that the waveplate is at 90° to the optical axis for all orientations of the optic axis (fast axis). In this section we tilt the mechanical holder 2.1° (Figure 8.b) to see if the optic axis of the crystal is tilted with respect to the polished surface OR if the waveplate is tilted in the mechanical holder. While the mechanical alignment of the waveplate with respect to

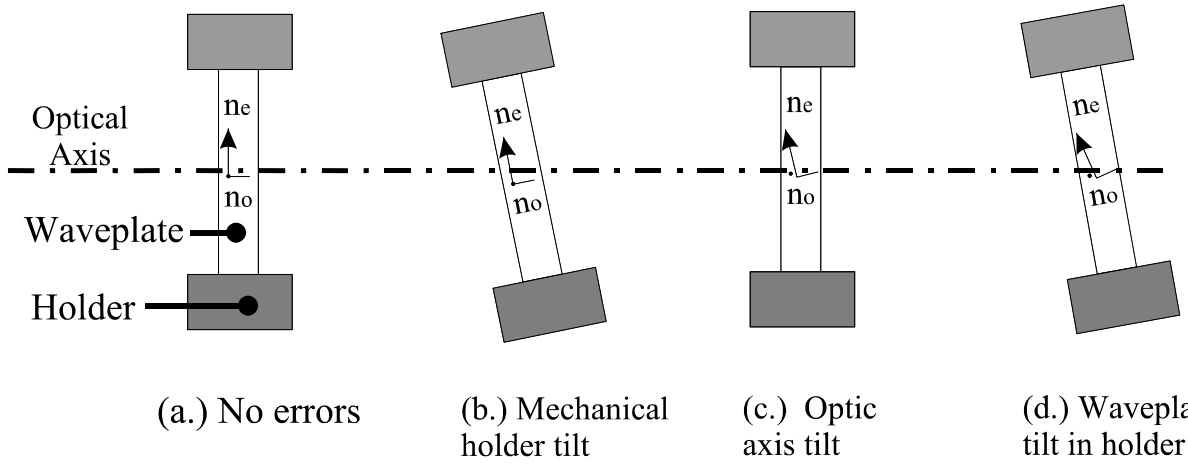

Figure 8. Waveplate alignment with respect to the optical axis.

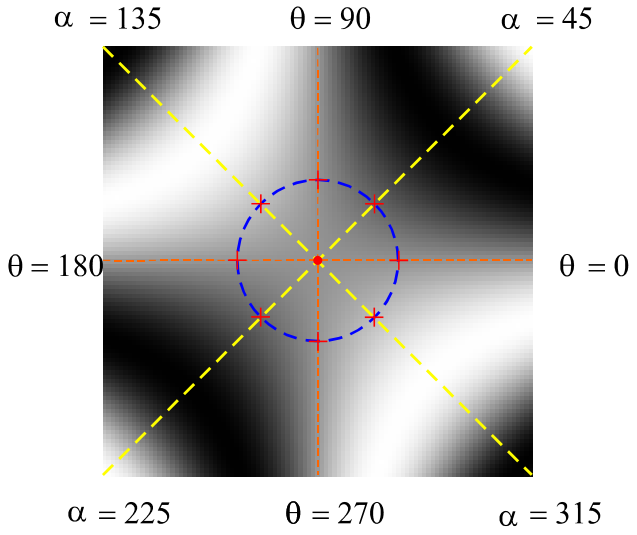

Figure 9. Intensity pattern that would be observed if the SUMI longitudinal waveplate was placed between crossed linear polarizers: wavelength 1550Å, field of view 10 degrees, input polarizer at θ=0° and the waveplate fast axis at α=45°.

the holder is checked when the waveplate is inserted into the test setup, the size of the reflected beam from the waveplate to the tilt calibration stop and the distance between these optical components limit the alignment accuracy to ~0.2°. Therefore, the errors introduced by the alignment errors in Figure 8.c and 8.d would have the same effect. The waveplate tilt of 2.1° was chosen because it is the same as the SUMI marginal ray. Therefore, the measured retardance at this angle will show how the retardance will vary over each pixel along the slit of the SUMI spectrograph. The dashed circle in Figure 9 represents the 2.1° tilt of the mechanical holder while the plus signs represent the different orientations that the holder will make with respect to the optical axis. These eight measurements will hopefully reduce the uncertainty between the optic axis tilt (Figure 8.c) and the wobble of the waveplate in the mechanical holder (Figure 8.d). The next section will describe the measurements and model required to fit the data.

4. Modeling waveplate errors

Since the retardance of a waveplate is dependent on several variables where small errors can be compensated for by the optician to obtain the specified "on-axis" retardance, modeling waveplate measurements is not exact and several solutions may exist. This section will discuss waveplate errors and how they affect the retardance measurement and the performance of the waveplate in the scientific instrument, in this case SUMI. In the previous section, different techniques were used to make retardation measurements on the same MgF_2 waveplate. Some of the "noise" in that data is related to alignment errors (Figure 8). Modeling the off-axis retardance measurements (Section 3.3) and fitting that data to a retardance versus wavelength model that has parameters for both the optic axis and optical axis tilt can reduce the errors bars on those measurements and produce a better understanding of how an instrument will respond to a particular waveplate.

4.1 Birefringence models

Initially the UV dual-polarimeter measurements were not available and the retardance measurements in the visible had to be extended into the UV to see if the waveplate met its design goal of 630° retardance at 1550Å. Three equations (Table 1) have been used to model the birefringence of MgF_2 and Figure 10 show the curve fits of those equations to the on-axis measurements of the SUMI waveplate. One of the reasons for developing the UV dual-polarimeter system was the uncertainty of extending these equations to cover this long wavelength range (1500-7500 Å). While published data of MgF_2 birefringence in the UV was used to develop the Zemax equation, it has flatter response in the visible. Therefore, the Karl Lambrecht coefficients were used to fit the visible light measurements.

Table 1. Coefficients to Sellmeier 1 equation for MgF_2 index of refraction.

Coefficient	Handbook of Optics		Karl Lambrecht		Zemax	
	n_o	n_e	n_o	n_e	n_o	n_e
b	0.48755108	0.41344023	0.48755108	0.41344023	0.498510062	0.488386509
c	0.04338408	0.03684262	0.04338408	0.03684262	0.002009353	0.002213759
d	0.39875031	0.50497499	0.39875031	0.50497499	0.387578137	0.42903173
e	0.09461442	0.09076162	0.09461442	0.09076162	0.009018453	0.00860767
f	2.3120353	2.4904862	2.3120353	2.4904862	1.0998616	-0.50652945
g	23.793604	12.771995	23.793604	23.771995	370.07139	400.982264

Sellmeier 1 formula $$\left(n_x\right)^2 - 1 := \frac{b\cdot\lambda^2}{\lambda^2 - c^2} + \frac{d\cdot\lambda^2}{\lambda^2 - e^2} + \frac{f\cdot\lambda^2}{\lambda^2 - g^2}$$ where x= o, e

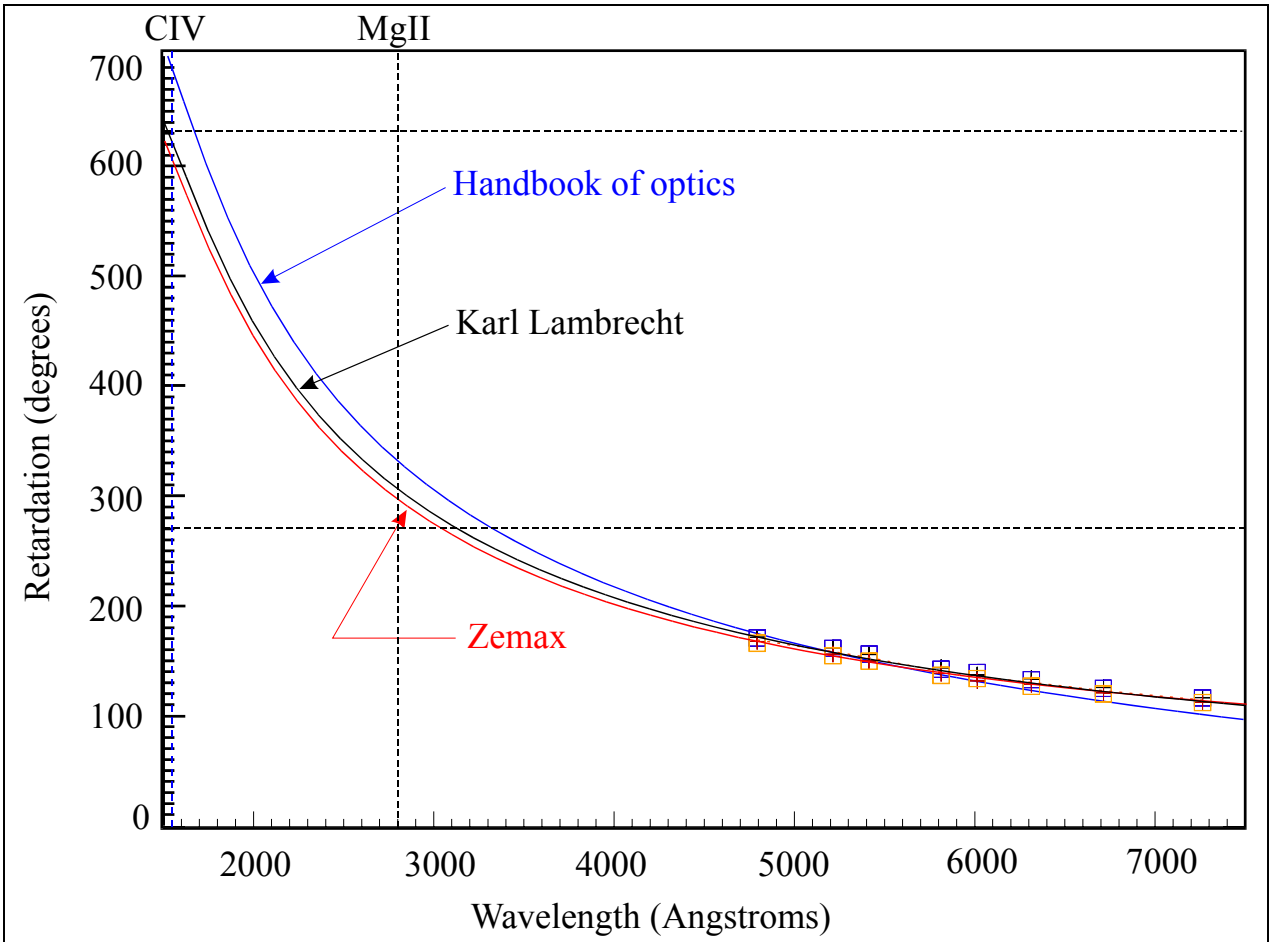

Figure 10. Modeling waveplate measurements using for MgF_2 indices of refraction from various sources. Curve A indices from Handbook of Optics (wavelength range: 2000-7040Å). Curve B from Karl Lambrecht (private communication). From Zemax optical design program[x] extended to UV wavelength range from published data[yz].

4.2 Curve fitting retardance measurements

Along with the uncertainties with the birefringence properties is the thickness of the two MgF_2 plates that make the SUMI longitudinal waveplate. Typically a waveplate's retardance is determined by the difference in the thickness of the two birefringent plates and the total thickness is kept small to minimize the field of view errors. Since the total thickness of the SUMI waveplate is approximately 2.3mm, the model assumes that the thickness of the first plate is 1.2mm and allows the thickness of the second plate to vary to obtain the observed retardance.

Along with the on-axis retardance measurements, the rotary stage holding the waveplate is tilted so that light reflected from the waveplate is 2.1° ± 0.2° from the optical axis of the test setup. The large uncertainty in the off-axis tilt is due to the large beam (~12.5mm) incident on the waveplate and the short distance between the waveplate and tilt calibration stop (~700mm). The main purpose of the off-axis measurements is to demonstrate how tilt errors affect the measured retardance (optical noise added to the electrical noise), how these errors limit the field of view of a waveplate and the effect of these errors in a scientific instrument such as SUMI.

Figure 11 shows the retardance measurements made on the SUMI longitudinal waveplate at four different angles of incidence. As expect the measured data for the four fast axis (FA) positions are on opposite sides of the average retardance (dashed line) when the tilt axes are on opposite sides of the optical axis (ie., top right and lower left). One point that is not obvious is the fact that the fast axis locations that should have the same retardance (ie., Figure 8.b, FA1=FA3 and FA2=FA4) are on opposite sides of the averaged retardance. The difference in the retardance at these locations is related a change in the tilt of the optic axis. Therefore, the difference in the parallel fast axis positions and the average retardance is used to fit the MgF2 birefringence to the retardance measurements.

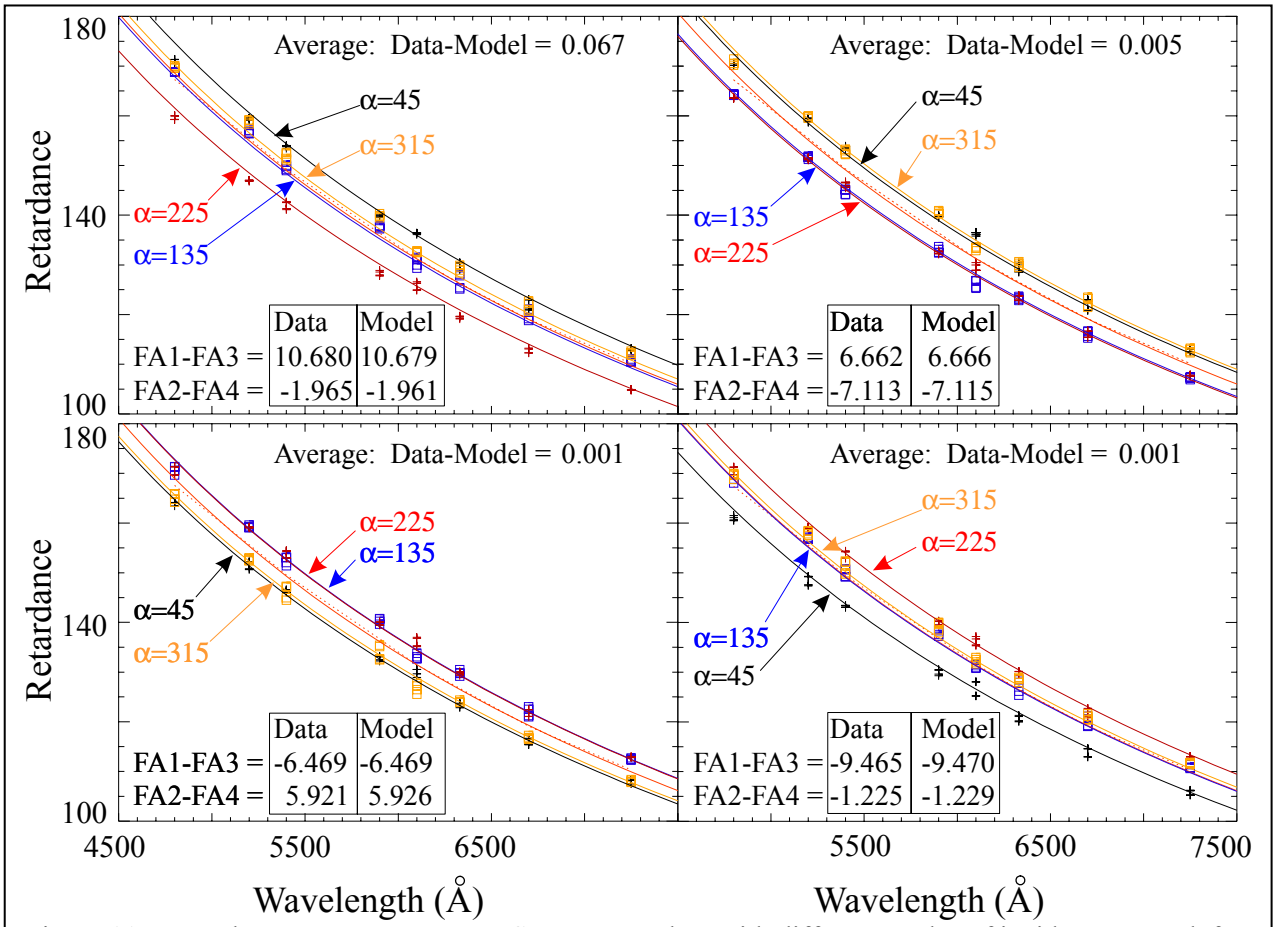

Figure 11. Retardance measurements on SUMI waveplate with different angles of incidence. Top left is a 1.05° AOI along the 90° axis in Figure 9, top right: 45° axis, bottom left: 225° axis and bottom right: 270° axis. At each tilt position the retardance of the waveplate is measured at the four fast axis (FA) positions. The fast axis positions are defined to be: FA1≡α=45°, FA2≡α=135°, FA3≡α=225° and FA4≡α=315°. The dashed line is the average of the measured retardance at the four FA positions while the overlapping solid line is the average FA positions from the curvefit (best seen in the top right and lower left plots).

Table 2. Summary of curve-fits to visible-light dual polarimeter retardance measurements on SUMI longitudinal waveplate (design goal: 630° @ 1550Å). The waveplate tilt axis is the mechanical tilt of the waveplate rotary stage along the axes define in Figure 9 (+ signs). Birefringence using the Karl Lambrecht coefficients (Table 1), retardance from curve fit at 1550Å, tilt angle with respect to optical axis is 1.05°. OA#1 is optic axis of first MgF_2 plate, OA#2 the second plate

Tilt axis (Figure 9)	Average Retardance	Retardance (degrees)	OA#1 tilt (degrees)	OA#2 tilt (degrees)
On-axis	622.98	624.71	0.764	0.564
0°	623.21	623.43	0.990	0.990
45°	622.68	630.30	1.302	0.723
90°	622.42	622.70	1.199	1.198
135°	623.60	616.65	0.713	1.279
180°	623.08	623.23	1.480	1.490
225°	623.45	631.05	1.217	0.558
270°	623.16	623.28	0.950	0.95
315°	622.94	611.39	0.547	1.469

Table 2 summarizes the retardance measurements made on the SUMI longitudinal waveplate. Since the waveplate was designed to be 630° at 1550Å the curvefits are extended to that wavelength. The average retardance of the four fast axis positions does not show a significant variation as the waveplate is tilted with respect to the optical axis. The retardance produced by the curvefits (column 3 in Table 2) shows a significant variation between the 45°/225° positions and the 135°/315° positions while there is small differences between the 0°/90°/180°/270° positions. These measurements also agree with the average retardance data. The explanation becomes obvious when these measurements are compared to the intensity patterns in Figure 9. This will become important when considering how this waveplate will influence the polarization measurements in SUMI.

4.3 Longitudinal measurements in SUMI

Although the intensity pattern in Figure 9 assumed that the waveplate is in a collimated beam, in order to reduce any loss from absorption the SUMI optical design does not have any refractive optics and the waveplate is placed near the focus of the telescope. With this design the incident beam on the waveplate is closer to a telecentric design than collimated. Therefore, the FOV errors at each point in the image plane of SUMI is the average retardance defined by the marginal ray. Since the chief ray angle for SUMI is small at the waveplate(~0.1°), the variation of the average retardance over the slit of the SUMI spectrograph will be small. The waveplate has been position ~100mm from the focus of the SUMI telescope to average out local polishing errors in the surface of the waveplate.

Figure 12 shows why the waveplate is much more sensitive to alignment errors at 1550Å than at visible wavelengths. For single-crystal, low-order waveplates, the polarization patterns in Figure 12 are simply related to the total thickness of the waveplate divided by the wavelength. Therefore, the only way to increase the field of view is to decrease the thickness.

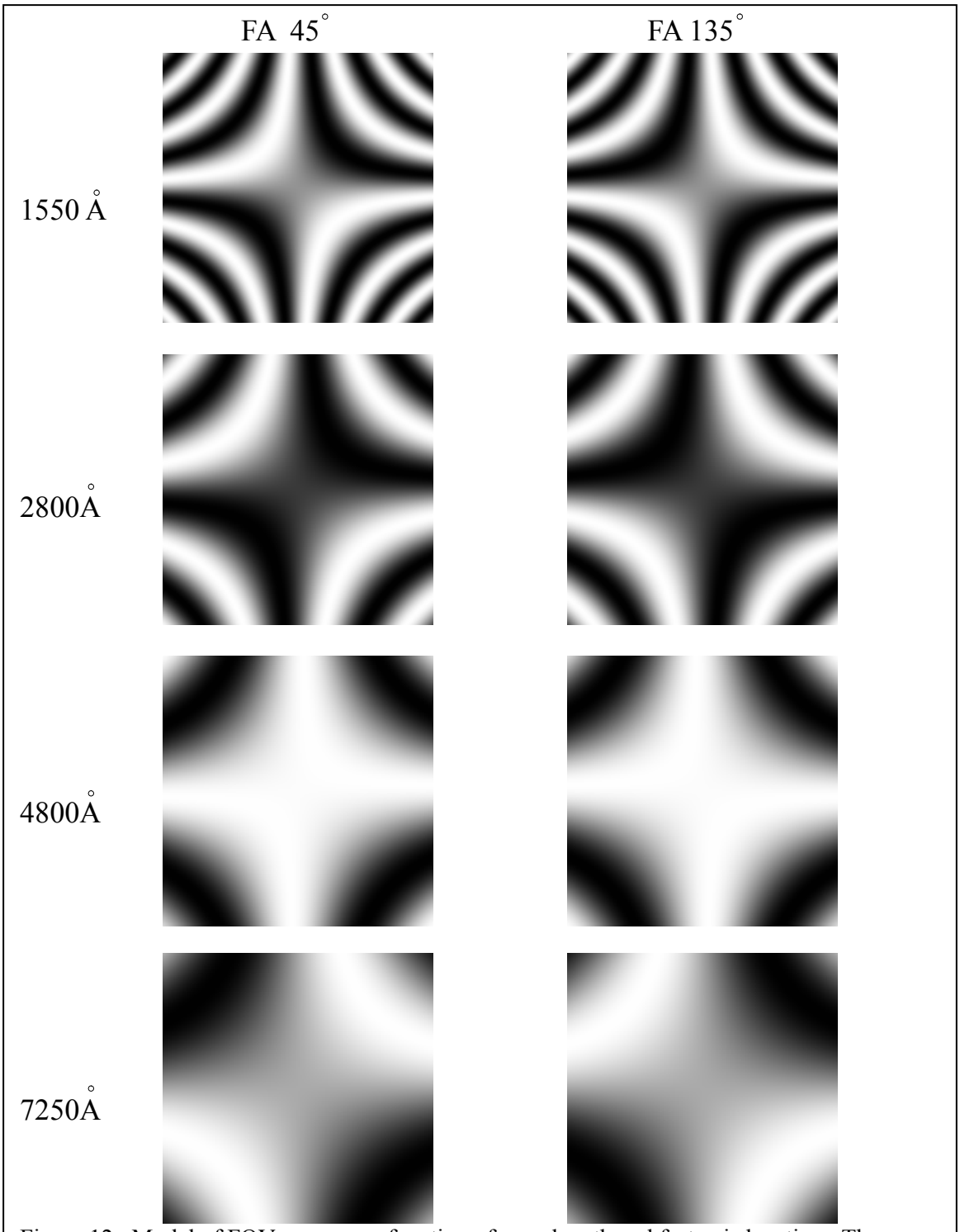

Figure 12. Model of FOV errors as a function of wavelength and fast axis location. The calculated field of view is ± 10° which is approximately four times the waveplate angle of incidence in the SUMI design (marginal ray= 2.3°, chief ray = .1°).

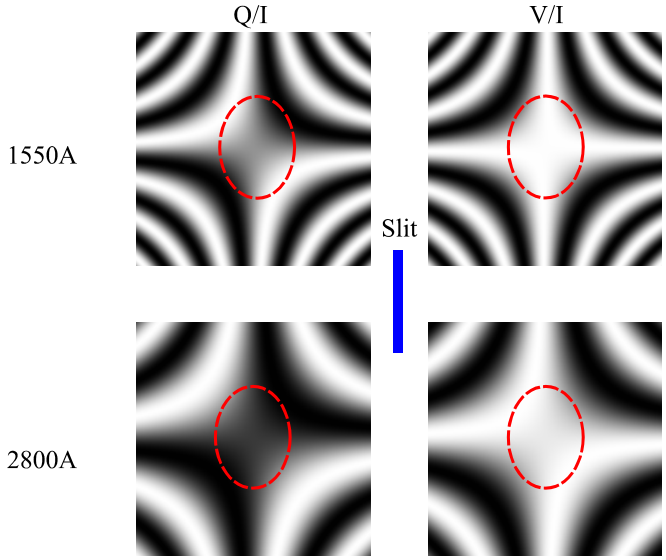

Figure 13. Footprint of the slit on the SUMI waveplate (dashed line on images). The ellipsoid shape is due to the length of the slit which is parallel (and pendicular) to the transmission axes of the double Wollaston analyzer.

While the marginal ray determines the variation of retardance, the alignment of SUMI spectrograph slit parallel (and perpendicular) to the transmission axis of the analyzer can reduce the large variations that were observed in Table 2.

In Figure 13, the orientation of the slit with respect to the analyzer transmission axis and the alignment of the optic axis/rotation axis of the waveplate with respect to the optical axis will determine the polarization efficiency and linear crosstalk (Q/I) in the circular polarization (V/I) measurement. The white cross pattern in the 1550Å measurement indicates that the waveplate is "quarterwave" while at 2800Å the cross shows a slight separation indicating a retardation error at this wavelength.

5. Summary

conclusions

1. **although the same waveplate is used, each fast axis position appears to be a different waveplate.**
2. **if there is no optic axis tilt, the parallel fast axis measurements should be the same (FA1: α=45° ↔ FA3: α=225° and FA2: α=135° ↔ FA4: α=315°)**
3. **Tilt errors parallel / perpendicular to the analyzer are not as critical as along the optic axis directions.**
4.

6. References

1. E. A. West and M. H. Smith, "Polarization Errors Associated with Birefringent Waveplates," Polarization Analysis and Measurement II, D. H. Goldstein and D. B. Chenault, eds., SPIE Vol. 2265, pp. 260-271 , 1994.
2. W. G. Driscoll, ed., "Handbook of Optics", New York: McGraw-Hill, Chapter 10, (1978).
3. E. A. West, J. G. Porter, J. M. Davis, G. A. Gary, and M. Adams, "Development of a polarimeter for magnetic field measurements in the ultraviolet", Polarization Analysis, Measurement, and Remote Sensing IV, D. Goldstein, D. Chenault, W. Egan, M. Duggin, eds., SPIE Vol. 4481, pp. 109-117, 2002.
4. D. L. Steinmetz, W. G. Phillips, M. Wirick and F. F. Forbes, "A Polarizer for the Vacuum Ultraviolet", Appl. Opt., Vol. 6, No. 6, pp. 1001-1004, June 1967.